

Bound states of the one-dimensional Schrödinger equation with arbitrary potential: a scattering matrix method

Carlos Ramírez^{1,3}, Fernanda H. Gonzalez¹ and César G. Galván²

¹ Departamento de Física, Facultad de Ciencias, Universidad Nacional Autónoma de México, Apartado Postal 70542, 04510 Ciudad de México, México

² Facultad de Ciencias, Universidad Autónoma de San Luis Potosí, Apartado Postal 78000 San Luis Potosí, México

³ Corresponding author e-mail: carlos@ciencias.unam.mx

Abstract

This paper presents an accurate highly efficient method for solving the bound states in the one-dimensional Schrödinger equation with an arbitrary potential. First, we demonstrate that the bound state energies of a general potential well can be obtained from the scattering matrices of two associated scattering potentials. Such scattering matrices can be determined with high efficiency and accuracy, leading us to a new method to find the bound state energies. Moreover, it allows to find the associated wavefunctions, their norm, and expected values. The method is validated by comparing solutions of the harmonic oscillator and the hydrogen atom with their analytical counterparts. The energies and eigenfunctions of a Lennard-Jones potential are also computed and compared to others reported in the literature. This method is highly parallelizable and produces results that reach machine precision with low computational effort.

Keywords: Bound states, Schrödinger equation, Scattering matrix, Lennard-Jones potential

1. Introduction

The physics of the one-dimensional systems has attracted the attention of the scientist in the last years because of the great number of applications in the optoelectronic and electronic. One-dimensional devices, such as FETs, diodes, photo-detectors, LEDs, etc, are of great importance in the development of technology and renewable energy [1]. The study of the one-dimensional quantum mechanics is the basis of all these devices.

The bound states of the well potential have been studied by using Airy functions [2] and Monte Carlo methods [3] leading to analytical solutions of specific potentials. On the other hand, the transfer matrix has been used to locally solve periodic potentials for different kind of waves [4][5], and the bound states can be treated as a tunneling problem by adding a barrier on both sides of the quantum well [6]. Other methods for solving arbitrary potentials use the transfer matrix where the potential well is divided into flat barriers [7][8] which allows to obtain better results than those given by the WKB approximation and variational calculations [9]. Such methods are also employed to find recursive solutions of the Schrödinger equation [10]. On the other hand, the scattering matrix method has been used to study the time dependent scattering of wave packets to obtain the bound states in one dimensional potentials. These include the step and two delta-function potentials [11], the square well potential [12] and those that use graphic constructions [13] on the bases of the Pitkanen method [14].

In a recent work [15], we propose a method to find the scattering states of an arbitrary potential in one dimension. In this method, the scattering region is divided in N smaller slices where the potential is approximated by polynomials. This method is highly accurate, numerically stable and requires low computational effort. In this work, we propose a new algorithm to exploit these advantages during calculations of scattering matrices and find the bound states of an arbitrary potential.

The article is organized in the following form. Section 2 describes the algorithm employed to find the bound states of a general potential well in terms of the scattering matrix of two associated potentials. In section 3 we validate this method by reproducing results of the quantum harmonic oscillator and the hydrogen atom. Finally, in section 4 we show how this method can be used to obtain the energies and normalized eigenfunctions of the Lennard-Jones potential.

2. The method

Let us start with a general one-dimensional potential well $V(x)$, as schematically shown in Fig. 1(a), with bound state energies E_n and wavefunctions $\psi_n(x)$. Let us define the following associated potentials

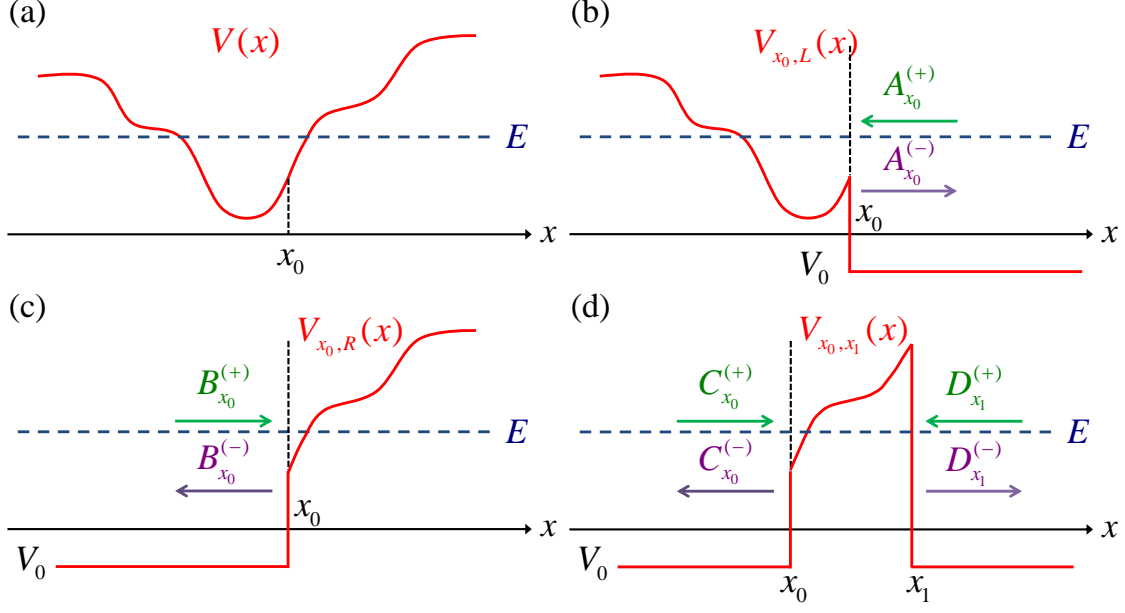


Figure 1. (a) General one-dimensional potential well. (b) Left associated potential. (c) Right associated potential. (d) Slice associated potential.

$$V_{x_0,L}(x) \equiv \begin{cases} V(x) & \text{if } x < x_0 \\ V_0 & \text{if } x \geq x_0 \end{cases}, \quad (1)$$

$$V_{x_0,R}(x) \equiv \begin{cases} V_0 & \text{if } x < x_0 \\ V(x) & \text{if } x \geq x_0 \end{cases}, \quad (2)$$

and

$$V_{x_0,x_1}(x) \equiv \begin{cases} V_0 & \text{if } x < x_0 \text{ or } x > x_1 \\ V(x) & \text{if } x_0 \leq x \leq x_1 \end{cases}, \quad (3)$$

with $V_0 < E$, as respectively illustrated in Fig. 1(b), 1(c) and 1(d).

Wavefunctions of potentials (1) to (3) are scattering states that can be written as

$$\psi_{x_0,L}(x) \equiv \begin{cases} \varphi(x) & \text{if } x \leq x_0 \\ A_{x_0}^{(+)} e^{-ik(x-x_0)} + A_{x_0}^{(-)} e^{ik(x-x_0)} & \text{if } x \geq x_0 \end{cases}, \quad (4)$$

$$\psi_{x_0,R}(x) \equiv \begin{cases} B_{x_0}^{(+)} e^{ik(x-x_0)} + B_{x_0}^{(-)} e^{-ik(x-x_0)} & \text{if } x \leq x_0 \\ \varphi(x) & \text{if } x \geq x_0 \end{cases}, \quad (5)$$

and

$$\psi_{x_0, x_1}(x) \equiv \begin{cases} C_{x_0}^{(+)} e^{ik(x-x_0)} + C_{x_0}^{(-)} e^{-ik(x-x_0)} & \text{if } x \leq x_0 \\ \varphi_{x_0, x_1}(x) & \text{if } x_0 \leq x \leq x_1 \\ D_{x_1}^{(+)} e^{-ik(x-x_1)} + D_{x_1}^{(-)} e^{ik(x-x_1)} & \text{if } x \geq x_1 \end{cases}, \quad (6)$$

respectively, where $k \equiv \sqrt{2m(E-V_0)}/\hbar$. Amplitude coefficients $(A_{x_0}^{(\pm)}, B_{x_0}^{(\pm)}, C_{x_0}^{(\pm)}$ and $D_{x_1}^{(\pm)})$ are related by the corresponding scattering matrices as follows

$$A_{x_0}^{(-)} = S_{x_0, L} A_{x_0}^{(+)}, \quad (7)$$

$$B_{x_0}^{(-)} = S_{x_0, R} B_{x_0}^{(+)} \quad (8)$$

and

$$\begin{pmatrix} C_{x_0}^{(-)} \\ D_{x_1}^{(-)} \end{pmatrix} = \mathbf{S}^{x_0, x_1} \begin{pmatrix} C_{x_0}^{(+)} \\ D_{x_1}^{(+)} \end{pmatrix} = \begin{pmatrix} S_{11}^{x_0, x_1} & S_{12}^{x_0, x_1} \\ S_{21}^{x_0, x_1} & S_{22}^{x_0, x_1} \end{pmatrix} \begin{pmatrix} C_{x_0}^{(+)} \\ D_{x_1}^{(+)} \end{pmatrix}. \quad (9)$$

Hereinafter, definitions of potentials, wavefunctions of scattering states, amplitude coefficients, and scattering matrices will follow the notation given in equations (1) to (9).

Notice that by setting $E = E_n$ and

$$A_{x_0}^{(\pm)} = B_{x_0}^{(\mp)} = \frac{ik\psi_n(x_0) \mp \psi_n'(x_0)}{2ik}, \quad (10)$$

continuity of wavefunction and its derivative imply $\varphi(x) = \psi_n(x)$ in Eqs. (4) and (5). In other words, scattering states of potentials (1) and (2) can be employed to describe bound states of potential $V(x)$.

Since wavefunctions $\psi_n(x)$ are bound states, they must have an evanescent behavior when $x \rightarrow \pm\infty$. In consequence, they are represented by total reflection states in equations (4) and (5), *i.e.*, $S_{x_0, L}$ and $S_{x_0, R}$ are phase factors. They can be independently calculated as functions of energy E . Consequently, there is a bound state of potential $V(x)$ at energy E if the first equality in Eq. (10) is satisfied, which imply

$$S_{x_0, L} S_{x_0, R} = 1. \quad (11)$$

In general, $S_{x_0, L} S_{x_0, R}$ is a unit complex number. Then, we can calculate eigenenergies of potential $V(x)$ by finding energies for which $\text{Im}(S_{x_0, L} S_{x_0, R}) = 0$ and discarding those with

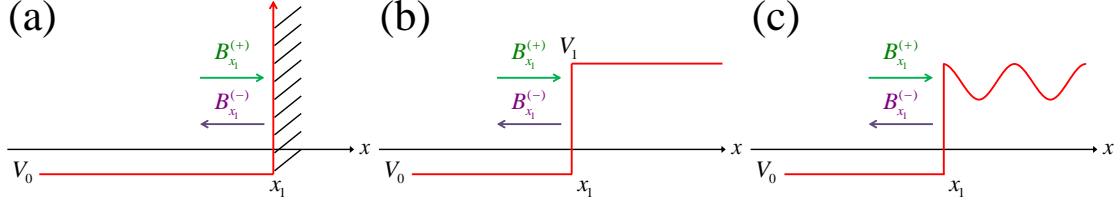


Figure 2. Potentials for which the phase change can be easily calculated: (a) an infinite potential barrier, (b) a potential step and (c) a semi-infinite periodic potential.

$\text{Re}(S^{x_0,L} S^{x_0,R}) = -1$. This can be done very efficiently by using secant or *regula falsi* methods. Next, we discuss how to calculate $S^{x_0,L}$, $S^{x_0,R}$ and wavefunctions $\psi_n(x)$.

2.1 Phase factors

Let us divide potential $V_{x_0,R}(x)$ in two independent potentials, $V_{x_0,x_1}(x)$ and $V_{x_1,R}(x)$. By using the method in Ref. [15], we can calculate the scattering matrix \mathbf{S}^{x_0,x_1} associated to potential $V_{x_0,x_1}(x)$. If $S^{x_1,R}$ is known, then by taking $D_{x_1}^{(\pm)} = B_{x_1}^{(\mp)}$, we obtain

$$S^{x_0,R} = \left(S_{11}^{x_0,x_1} + \frac{S_{12}^{x_0,x_1} S_{21}^{x_0,x_1} S^{x_1,R}}{1 - S_{x_1,R}^{x_1} S_{22}^{x_0,x_1}} \right). \quad (12)$$

There are several potentials for which $S^{x_1,R}$ can be exactly calculated, (a) the infinite potential barrier, (b) the step potential and (c) the semi-infinite periodic potential, which are illustrated in Fig. 2. The first two can be determined analytically to be respectively

$$S_{\text{barrier}}^{x_1,R} = -1, \quad (13)$$

and

$$S_{\text{step}}^{x_1,R} = \frac{ik + \kappa}{ik - \kappa}, \quad (14)$$

where $\kappa \equiv \sqrt{2m(V_1 - E)}/\hbar$ and $E < V_1$. On the other hand, the scattering matrix for the semi-infinite periodic potential can be calculated from the scattering matrix of its unit cell [16].

If $S^{x_1,R}$ is not known, notice that for x_1 big enough, the evanescent behavior of the wavefunction imply that $|S_{12}^{x_0,x_1}| < \varepsilon \ll 1$, and then

$$C_{x_0}^{(-)} = S_{11}^{x_0,x_1} C_{x_0}^{(+)} + S_{12}^{x_0,x_1} D_{x_1}^{(+)} \approx S_{11}^{x_0,x_1} C_{x_0}^{(+)}, \quad (15)$$

i.e., $S^{x_1, R} \approx S_{11}^{x_0, x_1}$. Since the method in Ref. [15] allow us to iteratively increase the value of x_1 , we can always make ε as small as desired.

An analogous procedure may be followed to obtain $S^{x_0, L}$ of potential $V_{x_0, L}(x)$.

2.2 Wavefunctions

Given an eigenenergy E_n of potential $V(x)$ and the phase factor $S^{x_0, R}$, let us consider potential $V_{x_0, \tilde{x}-\Delta}(x)$ with $\Delta \ll 1$ and $\tilde{x} > x_0$.

Eigenfunctions of the Schrodinger equation with potential $V_{x_0, \tilde{x}-\Delta}(x)$ can be written for $-\Delta \leq x - \tilde{x} \leq \Delta$ as [15]

$$\psi_n(x) = \alpha_+ \psi_+(x) + \alpha_- \psi_-(x). \quad (16)$$

Functions $\psi_{\pm}(x)$ can be expressed as

$$\psi_{\pm}(x) = e^{\pm i \sqrt{v_0}(x-\tilde{x})} \sum_{\lambda=0}^{\Lambda} \varphi_{\lambda}^{(\pm)} (x-\tilde{x})^{\lambda}, \quad (17)$$

where $\varphi_0^{(\pm)} = 1$, $\varphi_1^{(\pm)} = \varphi_2^{(\pm)} = 0$, and other coefficients $\varphi_{\lambda}^{(\pm)}$ are recursively obtained as

$$\varphi_n^{(\pm)} = \mp \frac{2i\sqrt{v_0}}{n} \varphi_{n-1}^{(\pm)} - \frac{1}{n(n-1)} \left(v_{n-2} + \sum_{\lambda=3}^{n-3} \varphi_{\lambda}^{(\pm)} v_{n-\lambda-2} \right). \quad (18)$$

In Eq. (18), v_n is obtained from the Taylor's expansion

$$\frac{2m[E - V(x)]}{\hbar^2} \equiv \sum_{\mu=0}^M v_{\mu} (x-\tilde{x})^{\mu}, \quad (19)$$

which may be exactly calculated by using automatic differentiation [17]. Even though $\Lambda = M = \infty$, since $\Delta \ll 1$, finite values of Λ and M are enough to reach machine precision during evaluation of wavefunctions.

On the other hand, by using Eq. (8) we have

$$C_{x_0}^{(+)} = A \quad \text{and} \quad C_{x_0}^{(-)} = S^{x_0, R} A, \quad (20)$$

where A is a constant. From Eq. (20) and the scattering matrix $(S^{x_0, \tilde{x}-\Delta})$ of potential $V_{x_0, \tilde{x}-\Delta}(x)$, we obtain

$$D_{\tilde{x}-\Delta}^{(+)} = \frac{S^{x_0, R} - S_{11}^{x_0, \tilde{x}-\Delta}}{S_{12}^{x_0, \tilde{x}-\Delta}} A, \quad (21)$$

and

$$D_{\tilde{x}-\Delta}^{(-)} = S_{21}^{x_0, \tilde{x}-\Delta} A + S_{22}^{x_0, \tilde{x}-\Delta} D_{\tilde{x}-\Delta}^{(+)} . \quad (22)$$

Moreover, by using continuity of wavefunction and its derivative at $x = \tilde{x} - \Delta$, we have

$$\begin{pmatrix} \psi_+(\tilde{x}-\Delta) & \psi_-(\tilde{x}-\Delta) \\ \psi'_+(\tilde{x}-\Delta) & \psi'_-(\tilde{x}-\Delta) \end{pmatrix} \begin{pmatrix} \alpha_+ \\ \alpha_- \end{pmatrix} = \begin{pmatrix} D_{\tilde{x}-\Delta}^{(-)} + D_{\tilde{x}-\Delta}^{(+)} \\ ik(D_{\tilde{x}-\Delta}^{(-)} - D_{\tilde{x}-\Delta}^{(+)}) \end{pmatrix}. \quad (23)$$

Hence, solving Eq. (23), by using Eqs. (17), (21) and (22), and substituting into Eq. (16) allow us to find an expansion of the wavefunction $\psi_n(x)$. In practice, this expansion is given in terms of a product of exponential and a truncated series of degree Λ , reaching machine precision if Λ is large enough. Moreover, changing the value of \tilde{x} allow us to write the wavefunction, $\psi_n(x)$, as a piecewise function. It is important to mention that this method to find wavefunctions is valid as long as

$$|S^{x_0, R} - S_{11}^{x_0, \tilde{x}-\Delta}| > \tilde{\varepsilon} \quad (24)$$

with $\tilde{\varepsilon}$ greater than machine precision. Otherwise, Eq. (21) may lead to numerical errors.

Piecewise expressions of $\psi_n(x)$ also allow us to determine its norm easily. By substituting exponential function in Eq. (17) with its Taylor expansion, $\psi_{\pm}(x)$ can be written as a truncated series of degree Λ . Consequently, $\psi_n(x)$ and $|\psi_n(x)|^2$ may also be written as truncated series of degree Λ , which are easy to integrate. Finally, the norm can be obtained by doing a piecewise integration of $|\psi_n(x)|^2$. An analogous procedure can be followed to calculate expected values.

The previous procedure allows us to find the wavefunction and its norm for $x > x_0$. An analogous process may be followed to obtain those with $x < x_0$.

2.3 Symmetric potentials

For $V(x) = V(-x)$ and $x_0 = 0$, we have $S^{0, R} = S^{0, L}$. Then equation (11) imply that $(S^{0, R})^2 = 1$.

Consequently, there is a bound state when

$$\text{Im}(S^{0, R}) = 0. \quad (25)$$

It is worth mentioning that in such zeroes, $\text{Re}(S^{0,R})$ is equal to 1 or -1 , which correspond to bound states with even or odd wavefunctions, respectively.

3. Method validation

The one-dimensional harmonic oscillator and the hydrogen atom are two well-known potentials with analytical energies and eigenfunctions [18][19]. We use these potentials to obtain energies and eigenfunctions by using the method in Sect. 2, and to compare them with their analytical counterparts.

3.1 Harmonic Oscillator

The harmonic oscillator, with Hamiltonian

$$\hat{H} = \frac{\hat{p}^2}{2m} + \frac{1}{2}m\omega^2\hat{x}^2, \quad (26)$$

has a symmetric potential. Fig. 3(a) shows imaginary (blue solid line) and real (red dashed line) parts of $S^{0,R}$ as a function of energy E . Calculation of $S^{0,R}$ was done as in Eq. (15) with x_1 big enough to make $|S_{12}^{0,x_1}| < \varepsilon$. To this end, the scattering matrix $\mathbf{S}^{0,2m\Delta}$ ($m=1,2,\dots$) was determined iteratively using the method in Ref. [15]. Fig. 3(a) was obtained by taking $\varepsilon=10^{-80}$, $\Delta=0.1$, $\Lambda=10$ and $M=2$. Observe that $\text{Im}(S^{0,R})=0$ around the eigenenergies of the harmonic oscillator $E_n^{\text{exact}} = \hbar\omega(n + \frac{1}{2})$, shown as yellow open circles in Fig. 3(a). Also notice that the behavior of $\text{Im}(S^{0,R})$ could be well approximated by straight lines around such zeroes. This fact allows us to find accurate approximations of energies, E_n , in a few iterations of secant or *regula falsi* methods. Fig. 3(b) illustrates the computational time and relative error obtained during calculations of E_9 ,

$$\text{Relative Error} \equiv \left| \frac{E_9 - E_9^{\text{exact}}}{E_9^{\text{exact}}} \right|, \quad (27)$$

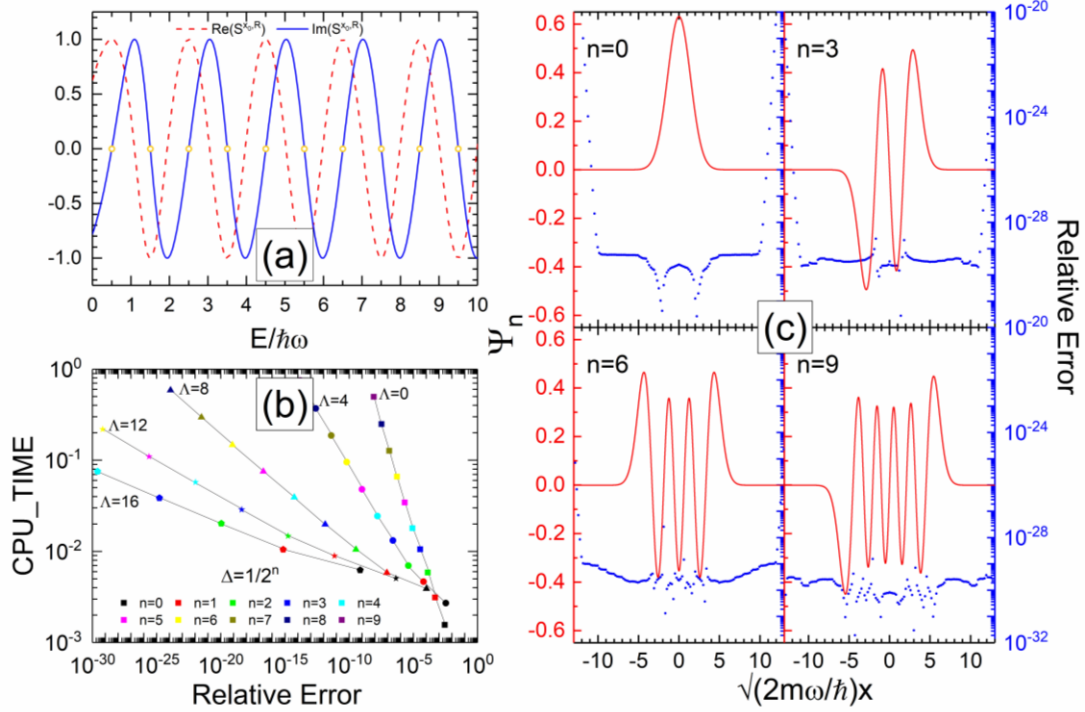


Figure 3. (a) Calculated imaginary (blue solid line) and real (red dashed line) parts of $S^{0,R}$ as functions of energy E for the quantum harmonic oscillator. (b) Computational time in arbitrary units versus relative error during calculations of the 9th excited state for different values of Δ and Λ . (c) Calculated wavefunctions (red solid line) and its relative error (blue dots) for $n=0,3,6$ and 9 .

when the secant method is applied, starting with initial values at $9.3\hbar\omega$ and $9.6\hbar\omega$, $\varepsilon=10^{-80}$, $M=2$, and different values of Δ and Λ . These calculations were done using quadruple precision arithmetic, which gives roughly 34 significant figures. Observe that precision is improved by increasing Λ or decreasing Δ , approaching rapidly machine precision when Λ is bigger. On the other hand, Fig. 3(c) shows the normalized wavefunctions calculated using the method in Section 2 with energies E_0 , E_3 , E_6 and E_9 (red solid lines), and the relative error (blue dots) when we compare them to the exact ones. Observe the excellent agreement between calculated wavefunctions and their analytical counterparts, with more than 28 significant figures of precision, except if $|x|$ is large, since here $|S^{x_0,R} - S_{11}^{x_0,\tilde{x}-\Delta}|$ becomes closer to machine precision.

3.2 Hydrogen atom

The hydrogen atom has a central potential, and its wavefunctions can be written as

$$\psi_{nlm}(r, \theta, \varphi) = \frac{u_{nl}(r)}{r} Y_l^m(\theta, \varphi). \quad (28)$$

The radial eigenfunction $u_{nl}(r)$ satisfies the one-dimensional Schrödinger equation,

$$-\frac{\hbar^2}{2m} \frac{\partial^2 u_{nl}(r)}{\partial r^2} + V_l(r) u_{nl}(r) = E_{nl} u_{nl}(r) \quad (29)$$

where $V_l(r)$ is the effective potential

$$V_l(r) = \frac{\hbar^2 l(l+1)}{2mr^2} - \frac{e^2}{4\pi\epsilon_0 r}. \quad (30)$$

Bound states in equation (28) have boundary conditions $u_{nl}(0) = 0$ and $\lim_{r \rightarrow \infty} u_{nl}(r) = 0$, and consequently $E_{nl} < 0$. Since there is a regular singularity at $r = 0$, a Frobenius series solution can be obtained, which lead us to analytical energies $E_n^{\text{exact}} = E_1/n^2$, where $n = l+1, l+2, l+3, \dots$, $E_1 \equiv -\hbar^2/2ma^2$ is the ground state energy, and a is the Bohr radius. However, in other cases, such as the Lennard-Jones potential presented in Sect. 4, Frobenius method is not suitable due to an essential singularity at $r = 0$. Hence, we take a different strategy to solve hydrogen atom that can be extended to more general cases. Firstly, note that if $l \geq 1$, the effective potential acts as an infinite barrier near $r = 0$. On the other hand, if r is big enough, the effective potential approximates a constant zero. Then, we may approximate potential (30) as

$$V_l^{\text{approx}}(r) = \begin{cases} \infty & \text{if } r < h_1 \\ \frac{\hbar^2 l(l+1)}{2mr^2} - \frac{e^2}{4\pi\epsilon_0 r} & \text{if } h_1 \leq r \leq h_2 \\ 0 & \text{if } h_2 < r \end{cases} \quad (31)$$

Figure 4(a) shows the imaginary (blue solid line) and real (red dashed line) parts of $S^{x_0, L} S^{x_0, R}$ for potential (31) with $l = 1$, $h_1 = 9.7844 \times 10^{-11} a$, $h_2 = 20200a$ by using the method in Sect. 2 with $x_0 = 2a$, $V_0 = 1.2E_1$, $M = 50$ and $\Lambda = M + 2$. Exact energies of Hydrogen atom are represented by yellow open circles. Following the method in Ref. [15], calculations were done by dividing potential in slices of variable-width $2\Delta_i$ with center at

points x_i . In Fig. 3 we use $\Delta_i = 0.01x_i$, which ensures that truncated Taylor expansions of potential inside each slice are exact within machine precision. Observe that $S^{x_0,L}S^{x_0,R} = 1$ around the exact energies. In fact, after using the secant root finding method, energies with at least 30 significant figures of precision are obtained for the first nine energies when calculations are done with quadruple precision arithmetic. Figure 4(b) shows the calculated normalized radial wavefunction $u_{41}(r)$ (red line) and the relative error (blue dots) when compared to the analytic exact one, by using the same parameters of Fig. 4(a).

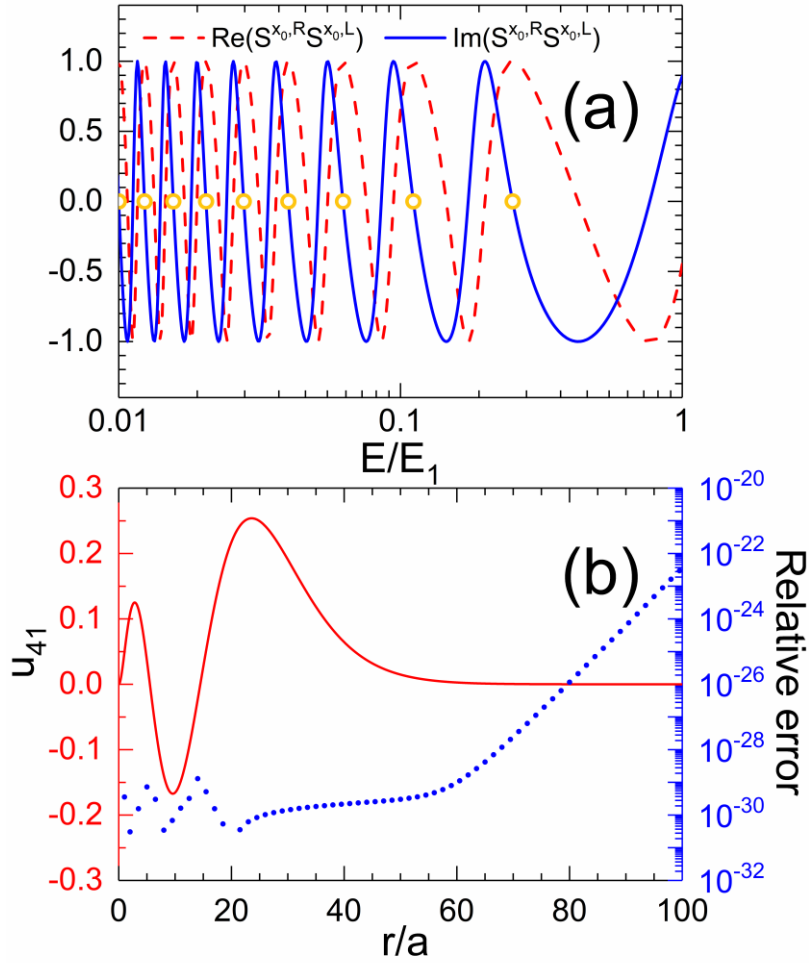


Figure 4. (a) Calculated imaginary (blue solid line) and real (red dashed line) parts of $S^{x_0,L}S^{x_0,R}$ as functions of energy E for the hydrogen atom with $l=1$ and $x_0=2a$. (b) Calculated radial wavefunction u_{41} (red solid line) and its relative error (blue dots).

4. Lennard-Jones potential

The radial Schrödinger equation for the Lennard-Jones potential, whose effective potential is

$$V_l(r) = \frac{\hbar^2 l(l+1)}{2mr^2} + 4\varepsilon \left[\left(\frac{\sigma}{r} \right)^{12} - \left(\frac{\sigma}{r} \right)^6 \right], \quad (32)$$

has an essential singularity at $r = 0$, which disallow us to find analytically its bound states. Observe that for any value of l , this potential acts as an infinite potential barrier around $r = 0$ and for large r it approximates a constant zero. Similarly to the hydrogen atom case, we then approximate effective potential (32) as

$$V_l^{approx}(r) = \begin{cases} \infty & \text{if } r < h_1 \\ \frac{\hbar^2 l(l+1)}{2mr^2} + 4\varepsilon \left[\left(\frac{\sigma}{r} \right)^{12} - \left(\frac{\sigma}{r} \right)^6 \right] & \text{if } h_1 \leq r \leq h_2 \\ 0 & \text{if } h_2 < r \end{cases} \quad (33)$$

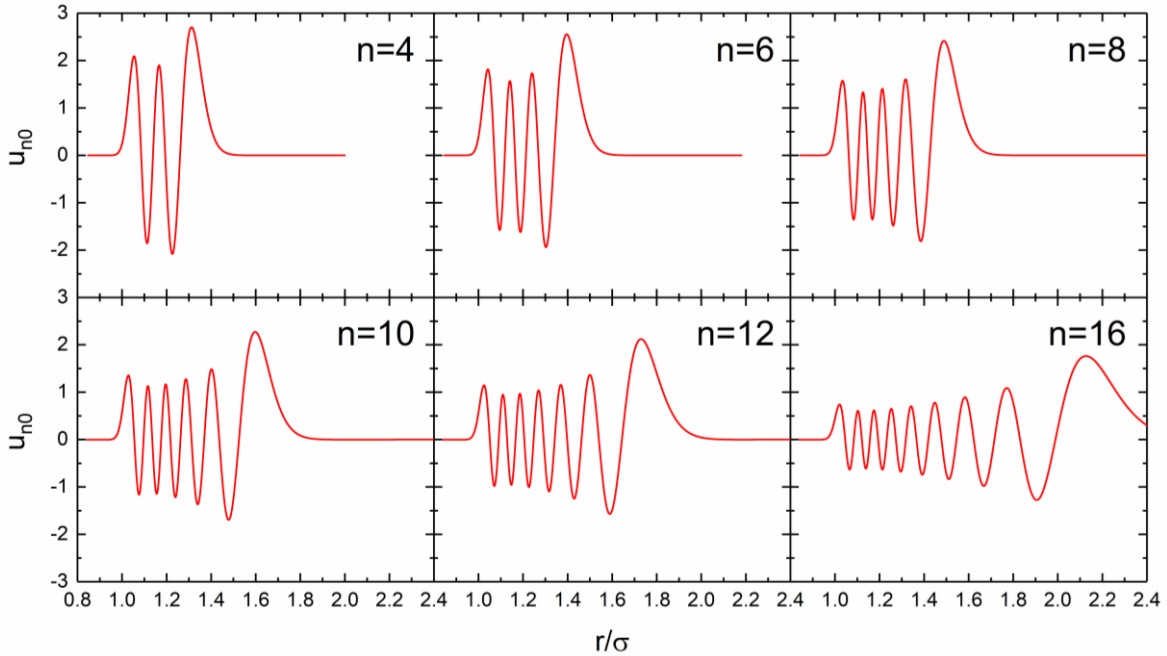


Figure 5. Calculated $l=0$ radial eigenfunctions $u_{n,0}$ of Lennard-Jones potential with $\varepsilon = 10^4 \hbar^2 / 2^{\frac{4}{3}} m \sigma^2$.

Table 1. Calculated energy (E_{n_0}), radial expected value ($\langle r \rangle$) and standard deviation (σ_r) of the first twenty levels of Lennard-Jones potential with $\varepsilon = 10^4 \hbar^2 / 2^{\frac{4}{3}} m \sigma^2$ and $l = 0$. This potential was approximated by that in Eq. (33) with $h_1 = 0.22\sigma$, $h_2 = 200\sigma$. Energies are presented for calculations using Double (DP) and Quadruple (QP) precision arithmetic.

n	DP E_{n_0}/ε	QP E_{n_0}/ε	$\langle r \rangle/\sigma$	σ_r/σ
0	-0.941046032004322	-0.94104603200432254854169387438	1.13250763	0.03332738
1	-0.830002082985871	-0.83000208298587138618852277327	1.15362644	0.05845972
2	-0.727645697519941	-0.72764569751994058057501425600	1.17638781	0.07714456
3	-0.633692951881524	-0.63369295188152437965217560942	1.20099976	0.09349374
4	-0.547852043328306	-0.54785204332830568209973511651	1.22770757	0.10872536
5	-0.469822910169227	-0.46982291016922668131723659309	1.25680268	0.12341928
6	-0.399296840303147	-0.39929684030314650876169900910	1.2886344	0.13792451
7	-0.335956071146719	-0.33595607114671895154568999297	1.32362541	0.15248893
8	-0.279473385016170	-0.27947338501616976487010617047	1.36229270	0.16731436
9	-0.229511705458584	-0.22951170545858385718317505171	1.40527636	0.18258579
10	-0.185723701795511	-0.18572370179551076878309561874	1.45337996	0.19849100
11	-0.147751411297187	-0.14775141129718670720790102414	1.50762849	0.21523776
12	-0.115225890997835	-0.11522589099783490602079612404	1.56935372	0.23307297
13	-0.087766914228358	-0.08776691422835835116924172300	1.64032393	0.25230831
14	-0.064982730496227	-0.06498273049622665020918574396	1.72294802	0.27335898
15	-0.046469911357580	-0.04646991135757998007579241010	1.82061078	0.29680714
16	-0.031813309315001	-0.03181330931500057799809844862	1.93825223	0.32351356
17	-0.020586161355897	-0.02058616135589709812351189413	2.08343401	0.35482959
18	-0.012350373215634	-0.01235037321563388754785482702	2.26846612	0.39303815
19	-0.006657024343754	-0.00665702434375368196884511349	2.51512233	0.44239045

Table 1 shows the lowest twenty calculated energies of Schrodinger equation with potential (33) obtained by using double and quadruple precision arithmetic, with $l = 0$, $h_1 = 0.22\sigma$, $h_2 = 200\sigma$, $\varepsilon = 10^4 \hbar^2 / 2^{\frac{4}{3}} m \sigma^2$, $x_0 = 2^{1/6} \sigma$, $V_0 = -1.1\varepsilon$, $M = 50$ and $\Lambda = M + 2$. Potential was divided in slices with center at points x_i and width $2\Delta_i = 0.002x_i$. Cases with $n = 4, 6, 8, 10, 12$ and 16 are in full agreement with those reported by B.D. Shizgal [20]. Observe that eigenvalues calculated with double precision arithmetic are accurate with at

least 14 significant figures when compared to those obtained using quadruple precision arithmetic, showing the numerical stability of this method. Table 1 also presents the radial expected value $\langle r \rangle$ and standard deviation σ_r of the related wavefunction. As expected, wavefunctions with bigger energy have higher $\langle r \rangle$ and more delocalized wavefunctions, due to a greater turning point. This can also be noticed in Figure 5, which displays normalized radial eigenfunctions, $u_{n,0}$, for the cases of $n = 4, 6, 8, 10, 12$ and 16 .

5. Discussion and conclusions

In this work we have presented a novel method to solve eigenpairs of the one-dimensional Schrödinger equation with an arbitrary potential well based on accurate calculations of scattering matrices of its subsystems. The method starts by dividing a general potential well in two independent scattering problems, represented by the left and right associated potentials in Fig. 1. The scattering matrices of these potentials are phase changes and, as explained in Sect. 2.1, are accurately calculated by using the method in Ref. [15]. We have an energy of the potential well when the product of scattering matrices of these associated systems is one. Then we scan the results of this product as function of energy, as in Fig. 4(a), to determine where its imaginary part changes of sign and its real part approaches one. Observe that this scanning may be done for a selected range of energies of interest, avoiding wasting of time from computing other energies. It also allows parallelization, since different processors may scan different ranges of energies. Then a *regula falsi* or a secant method is applied to determine with higher precision the energy for which the imaginary part of this product becomes zero. This process is also parallelizable, since the precision refinement can be done on each energy by a different processor. Moreover, this refinement process can be optimized, by increasing progressively the precision arithmetic. For example, in table 1, double precision results are seeds to calculate quadruple precision ones, taking advantage of the reduced computational time during double precision calculations. If needed, quadruple precision results may be also used as seeds on extended precision calculations.

The method allows us to obtain the wavefunctions as piecewise functions, which also allow a direct computation of expected values. Since equation (21) is susceptible to numerical error, quadruple precision arithmetic is recommended during calculations of the normalized wavefunction. Comparison to wavefunctions of quantum harmonic oscillator and hydrogen atom showed in Figs. 3(c) and 4(b), illustrate the accuracy of this method, with more than 28 significant figures of precision. Results obtained for the Lennard-Jones potential also reflect excellent agreement when compared to other state of the art methods [20].

In summary, the proposed method to solve energies and wavefunctions of the one-dimensional Schrödinger equation with an arbitrary potential well is highly efficient, parallelizable, accurate and easy to implement.

Acknowledgments

This work has been supported by UNAM-DGAPA-PAPIIT IA106617. Computations were performed at Miztli under project LANCAD-UNAM-DGTIC-329.

References

- [1] G. Shen, D. Chen, *Front. Optoelectron. China* 3 (2010) 125-138.
- [2] A.K. Ghatak, R.L. Gallawa, I.C. Goyal, *IEEE J. Quantum Electron.* 28 (1992) 400.
- [3] J. Singh, *Appl. Phys. Lett.* 48 (1986) 434.
- [4] D.J. Griffiths, N.F. Taussig, *Am. J. Phys.* 60 (1992) 883-888.
- [5] D.J. Griffiths, Carl A. Steinke, *Am. J. Phys.* 69 (2001) 137-154.
- [6] M. Bosken, A.Seller, B. Waring, M. Cahay, *Physica E* 64 (2014) 141-145.
- [7] T.M. Kalotas, A.R. Lee, *Am. J. Phys.* 59 (1991) 48-51.
- [8] T.M. Kalotas, A.R. Lee, *Am. J. Phys.* 59 (1991) 1036-1038.
- [9] B. Jonsson, S.T. Eng, *IEEE J. Quantum Electron.* 26 (1990) 2015-2035.
- [10] H. Lee, Y. Lee, *J. Phys. A: Math. Theor* 40 (2007) 3569-3581.
- [11] C.L. Hammer, T.A. Weber, V.S. Zidell, *Am. J. Phys.* 45 (1977) 933.
- [12] T.A. Weber, C.L. Hammer, V.S. Zidell, *Am. J. Phys.* 50 (1982) 839.
- [13] D.W.L. Sprung, H. Wu, J. Martorell, *Am. J. Phys.* 64 (1996) 136.
- [14] D.W.L. Sprung, H. Wu, J. Martorell, *Eur. J. Phys.* 13, (1992) 21-25.

- [15] C. Ramírez, R. León, J. Phys. Soc. Jpn. 86 (2017) 114002.
- [16] C. Ramírez, Ann. Phys. (Berlin) 530 (2018) 1700170.
- [17] K. Makino, M. Berz, IJPAM 4 (2003) 379-452.
- [18] D.J. Griffiths, second ed. Pearson Prentice Hall, 2005.
- [19] J.S. Townsend, A modern approach to quantum mechanics, second ed., University Science Books, 2012.
- [20] B.D. Shizgal, Comput. Theor. Chem. 1114 (2017) 25.